Published in Optics Express 26, issue 9, 12306-12317, 2018
which should be used for any reference to this work

Electrically-driven pure amplitude and frequency modulation in a quantum cascade laser

ATIF SHEHZAD,[1] PIERRE BROCHARD,[1] RENAUD MATTHEY,[1] STÉPHANE BLASER,[2] TOBIAS GRESCH,[2] RICHARD MAULINI,[2] ANTOINE MULLER,[2] THOMAS SÜDMEYER,[1] AND STÉPHANE SCHILT[1,*]

[1]*Laboratoire Temps-Fréquence, Université de Neuchâtel, Av. de Bellevaux 51, CH-2000 Neuchâtel, Switzerland*
[2]*Alpes Lasers SA, Av. des Pâquiers 1, CH-2072 Saint-Blaise, Switzerland*
**stephane.schilt@unine.ch*

Abstract: We present pure amplitude modulation (AM) and frequency modulation (FM) achieved electrically in a quantum cascade laser (QCL) equipped with an integrated resistive heater (IH). The QCL output power scales linearly with the current applied to the active region (AR), but decreases with the IH current, while the emission frequency decreases with both currents. Hence, a simultaneous modulation applied to the current of the AR and IH sections with a proper relative amplitude and phase can suppress the AM, resulting in a pure FM, or vice-versa. The adequate modulation parameters depend on the applied modulation frequency. Therefore, they were first determined from the individual measurements of the AM and FM transfer functions obtained for a modulation applied to the current of the AR or IH section, respectively. By optimizing the parameters of the two modulations, we demonstrate a reduction of the spurious AM or FM by almost two orders of magnitude at characteristic frequencies of 1 and 10 kHz compared to the use of the AR current only.

OCIS codes: (140.5965) Semiconductor lasers, quantum cascade; (140.3518) Lasers, frequency modulated; (300.6380) Spectroscopy, modulation.

References and links

1. J. M. Supplee, E. A. Whittaker, and W. Lenth, "Theoretical description of frequency modulation and wavelength modulation spectroscopy," Appl. Opt. **33**(27), 6294–6302 (1994).
2. S. Schilt, L. Thévenaz, and P. Robert, "Wavelength Modulation Spectroscopy: Combined Frequency and Intensity Laser Modulation," Appl. Opt. **42**(33), 6728–6738 (2003).
3. G. C. Bjorklund, "Frequency-modulation spectroscopy: a new method for measuring weak absorptions and dispersions," Opt. Lett. **5**(1), 15–17 (1980).
4. R. Matthey, S. Schilt, D. Werner, C. Affolderbach, L. Thévenaz, and G. Mileti, "Diode laser frequency stabilisation for water-vapour differential absorption sensing," Appl. Phys. B **85**(2–3), 477–485 (2006).
5. R. W. P. Drever, J. L. Hall, F. V. Kowalski, J. Hough, G. M. Ford, A. J. Munley, and H. Ward, "Laser phase and frequency stabilization using an optical resonator," Appl. Phys. B **31**(2), 97–105 (1983).
6. E. D. Black, "An introduction to Pound–Drever–Hall laser frequency stabilization," Am. J. Phys. **69**(1), 79–87 (2001).
7. R. W. Fox, C. W. Oates, and L. W. Hollberg, "Stabilizing diode lasers to high-finesse cavities," in *Experimental Methods in the Physical Sciences*, R. D. van Zee and J. P. Looney, eds., Cavity-Enhanced Spectroscopies (Academic Press, 2003), Vol. 40, pp. 1–46.
8. M. W. Sigrist, "Trace gas monitoring by laser photoacoustic spectroscopy and related techniques," Rev. Sci. Instrum. **74**(1), 486–490 (2003).
9. A. A. Kosterev, Y. A. Bakhirkin, R. F. Curl, and F. K. Tittel, "Quartz-enhanced photoacoustic spectroscopy," Opt. Lett. **27**(21), 1902–1904 (2002).
10. S. Schilt and L. Thévenaz, "Experimental method based on wavelength-modulation spectroscopy for the characterization of semiconductor lasers under direct modulation," Appl. Opt. **43**(22), 4446–4453 (2004).
11. A. Hangauer, J. Chen, R. Strzoda, and M. C. Amann, "The Frequency Modulation Response of Vertical-Cavity Surface-Emitting Lasers: Experiment and Theory," IEEE J. Sel. Top. Quantum Electron. **17**(6), 1584–1593 (2011).

Optics EXPRESS

12. A. J. McGettrick, K. Duffin, W. Johnstone, G. Stewart, and D. G. Moodie, "Tunable Diode Laser Spectroscopy With Wavelength Modulation: A Phasor Decomposition Method for Calibration-Free Measurements of Gas Concentration and Pressure," J. Lightwave Technol. **26**(4), 432–440 (2008).
13. D. T. Cassidy and J. Reid, "Atmospheric pressure monitoring of trace gases using tunable diode lasers," Appl. Opt. **21**(7), 1185–1190 (1982).
14. S. Schilt, A. A. Kosterev, and F. K. Tittel, "Performance evaluation of a near infrared QEPAS based ethylene sensor," Appl. Phys. B **95**(4), 813–824 (2009).
15. P. Patimisco, A. Sampaolo, Y. Bidaux, A. Bismuto, M. Scott, J. Jiang, A. Muller, J. Faist, F. K. Tittel, and V. Spagnolo, "Purely wavelength- and amplitude-modulated quartz-enhanced photoacoustic spectroscopy," Opt. Express **24**(23), 25943–25954 (2016).
16. A. Hangauer, G. Spinner, M. Nikodem, and G. Wysocki, "Chirped laser dispersion spectroscopy using a directly modulated quantum cascade laser," Appl. Phys. Lett. **103**(19), 191107 (2013).
17. D. D. Nelson, J. H. Shorter, J. B. McManus, and M. S. Zahniser, "Sub-part-per-billion detection of nitric oxide in air using a thermoelectrically cooled mid-infrared quantum cascade laser spectrometer," Appl. Phys. B **75**(2–3), 343–350 (2002).
18. D. M. Sonnenfroh, W. T. Rawlins, M. G. Allen, C. Gmachl, F. Capasso, A. L. Hutchinson, D. L. Sivco, J. N. Baillargeon, and A. Y. Cho, "Application of balanced detection to absorption measurements of trace gases with room-temperature, quasi-cw quantum-cascade lasers," Appl. Opt. **40**(6), 812–820 (2001).
19. K. Namjou, S. Cai, E. A. Whittaker, J. Faist, C. Gmachl, F. Capasso, D. L. Sivco, and A. Y. Cho, "Sensitive absorption spectroscopy with a room-temperature distributed-feedback quantum-cascade laser," Opt. Lett. **23**(3), 219–221 (1998).
20. S. Borri, S. Bartalini, P. De Natale, M. Inguscio, C. Gmachl, F. Capasso, D. L. Sivco, and A. Y. Cho, "Frequency modulation spectroscopy by means of quantum-cascade lasers," Appl. Phys. B **85**(2–3), 223–229 (2006).
21. B. A. Paldus, T. G. Spence, R. N. Zare, J. Oomens, F. J. M. Harren, D. H. Parker, C. Gmachl, F. Cappasso, D. L. Sivco, J. N. Baillargeon, A. L. Hutchinson, and A. Y. Cho, "Photoacoustic spectroscopy using quantum-cascade lasers," Opt. Lett. **24**(3), 178–180 (1999).
22. R. Lewicki, G. Wysocki, A. A. Kosterev, and F. K. Tittel, "QEPAS based detection of broadband absorbing molecules using a widely tunable, cw quantum cascade laser at 8.4 μm," Opt. Express **15**(12), 7357–7366 (2007).
23. B. A. Paldus, C. C. Harb, T. G. Spence, R. N. Zare, C. Gmachl, F. Capasso, D. L. Sivco, J. N. Baillargeon, A. L. Hutchinson, and A. Y. Cho, "Cavity ringdown spectroscopy using mid-infrared quantum-cascade lasers," Opt. Lett. **25**(9), 666–668 (2000).
24. L. Tao, K. Sun, D. J. Miller, M. A. Khan, and M. A. Zondlo, "Current and frequency modulation characteristics for continuous-wave quantum cascade lasers at 9.06 μm," Opt. Lett. **37**(8), 1358–1360 (2012).
25. A. Hangauer, G. Spinner, M. Nikodem, and G. Wysocki, "High frequency modulation capabilities and quasi single-sideband emission from a quantum cascade laser," Opt. Express **22**(19), 23439–23455 (2014).
26. C. Peng, H. Zhou, L. Zhu, T. Chen, Q. Liu, D. Wang, J. Li, Q. Peng, G. Chen, and Z. Li, "Purified frequency modulation of a quantum cascade laser with an all-optical approach," Opt. Lett. **42**(21), 4506–4509 (2017).
27. A. Bismuto, Y. Bidaux, C. Tardy, R. Terazzi, T. Gresch, J. Wolf, S. Blaser, A. Muller, and J. Faist, "Extended tuning of mid-ir quantum cascade lasers using integrated resistive heaters," Opt. Express **23**(23), 29715–29722 (2015).
28. K. Gürel, S. Schilt, A. Bismuto, Y. Bidaux, C. Tardy, S. Blaser, T. Gresch, and T. Südmeyer, "Frequency Tuning and Modulation of a Quantum Cascade Laser with an Integrated Resistive Heater," Photonics **3**(3), 47 (2016).
29. S. Schilt, L. Tombez, C. Tardy, A. Bismuto, S. Blaser, R. Maulini, R. Terazzi, M. Rochat, and T. Sudmeyer, "Frequency Ageing and Noise Evolution in a Distributed Feedback Quantum Cascade Laser Measured Over a Two-Month Period," IEEE J. Sel. Top. Quantum Electron. **21**(6), 68–73 (2015).
30. L. S. Rothman, I. E. Gordon, Y. Babikov, A. Barbe, D. Chris Benner, P. F. Bernath, M. Birk, L. Bizzocchi, V. Boudon, L. R. Brown, A. Campargue, K. Chance, E. A. Cohen, L. H. Coudert, V. M. Devi, B. J. Drouin, A. Fayt, J.-M. Flaud, R. R. Gamache, J. J. Harrison, J.-M. Hartmann, C. Hill, J. T. Hodges, D. Jacquemart, A. Jolly, J. Lamouroux, R. J. Le Roy, G. Li, D. A. Long, O. M. Lyulin, C. J. Mackie, S. T. Massie, S. Mikhailenko, H. S. P. Müller, O. V. Naumenko, A. V. Nikitin, J. Orphal, V. Perevalov, A. Perrin, E. R. Polovtseva, C. Richard, M. A. H. Smith, E. Starikova, K. Sung, S. Tashkun, J. Tennyson, G. C. Toon, V. G. Tyuterev, and G. Wagner, "The HITRAN2012 molecular spectroscopic database," J. Quant. Spectrosc. Radiat. Transf. **130**, 1304–1350 (2013).
31. A. L. Chakraborty, K. Ruxton, W. Johnstone, M. Lengden, and K. Duffin, "Elimination of residual amplitude modulation in tunable diode laser wavelength modulation spectroscopy using an optical fiber delay line," Opt. Express **17**(12), 9602–9607 (2009).

1. Introduction

A wide range of applications make use of modulated laser sources, notably in optical communications and sensing. Combining a modulation scheme with a demodulation (e.g., lock-in detection) generally leads to a strong improvement in the detection sensitivity. Different types of modulation schemes can be applied, depending on the involved sensor and

Optics EXPRESS

the parameter to be measured. The most common relate to modulation of the optical power (amplitude modulation – AM), of the optical frequency (frequency modulation – FM) or of the optical phase (phase modulation – PM). For instance, wavelength and frequency modulation spectroscopy (WMS/FMS) methods are widely used to detect small absorption features in trace gas laser spectroscopy sensing. They consist in modulating the wavelength/frequency of a laser and detecting the harmonic signals of an atomic or molecular transition obtained when the laser frequency is additionally scanned through the transition. It leads to the generation of derivative-like signals of the probed absorption profile in WMS [1,2] or to the possibility to access both the absorption and dispersion of a gaseous sample in FMS [3]. Odd-harmonic WMS signals like 1*f* or 3*f* are also commonly used to stabilize a laser onto a molecular or atomic transition [4]. The well-known Pound-Drever-Hall method [5] widely applied to narrow down the linewidth of a laser by frequency stabilization to a high-finesse optical cavity is one of the most important applications of FMS [6,7]. In a different area of gas sensing, light modulated at audio frequencies (in amplitude or wavelength) and absorbed in a gaseous sample can excite acoustic waves, which are exploited for sensitive trace gas monitoring in various photoacoustic spectroscopy (PAS) methods [8,9].

Semiconductor lasers are the most commonly used laser source in trace gas sensing applications owing to their unique properties like single-mode emission, wavelength tunability and fast modulation capabilities. They can easily be directly modulated via their injection current and up to high frequencies in the GHz range. However, both their emission frequency and output power vary with the injection current. Therefore, modulating the injection current results in combined AM-FM, with a phase shift between the two modulations that depends on the applied modulation frequency [10,11]. The residual amplitude modulation (RAM) can sometimes be exploited, for instance for the recovery of absolute absorption line shapes from the 1st harmonic WMS signal [12] or for power normalization of the WMS-2*f* signal (2*f*/1*f* ratio) in trace gas sensing [13]. However, RAM most often constitutes an undesired effect that distorts the harmonic signals in WMS. It leads to an asymmetry in the second-harmonic (2*f*) signal often used in trace gas monitoring [2] or to an offset in the first-harmonic (1*f*) signal that can be detrimental in laser frequency stabilization experiments by inducing a frequency shift of the locking point from the center of the transition. The third harmonic (3*f*) signal can be used to mitigate this effect as it is in principle offset-free; however, this signal is generally much weaker, especially if small modulation amplitudes are used, which may make this approach impracticable in practice [4]. Therefore, the use of a pure FM would be beneficial to these applications. On the other hand, pure AM is sometimes also desired, for instance in PAS sensing of broadband or non-structured absorption spectra [14] or even for narrow gas absorption lines in some cases [15], as well as in chirped laser dispersion spectroscopy [16].

Quantum cascade lasers (QCLs) are the most widespread laser source for high-resolution molecular spectroscopy and trace-gas sensing in the mid-infrared fingerprint spectral region. They have been widely deployed with the most sensitive spectroscopic techniques, such as long-path length [17], balanced detection [18], WMS [19], FMS [20], PAS or quartz-enhanced PAS [21,22], cavity ring-down spectroscopy [23] and chirped laser dispersion spectroscopy [16]. Similar to near-infrared laser diodes, a modulation applied to their injection current results in combined AM and FM [24,25]. Different approaches have been studied in the last years to generate a pure FM (or pure AM in some cases) from a QCL. A first approach for pure FM was realized optically by simultaneously illuminating the front facet of a QCL by two continuous-wave near-infrared laser sources of different wavelengths (1.55 µm and 850 nm), corresponding to photon energies smaller and higher, respectively, than the edge of the electrons energy sub-band [26]. Both incident laser beams produced a blue shift of the QCL wavelength as a result of the induced change of the carrier density, whereas they yielded AM of opposite sign. AM was thus efficiently suppressed by proper adjustment of the incident modulated powers, leading to pure FM.

Optics EXPRESS

Another method to produce pure FM or AM was demonstrated in a quartz-enhanced PAS sensor using a special QCL structure made of three independent sections [15]. The master oscillator (i.e., the lasing section), the gain section (amplifier) and the phase section were controlled by distinct electrical currents. The phase section enabled controlling the reflectivity of the front facet of the QCL by adjusting the reflection phase, thus strongly affecting the emitted optical power. A combination of currents selectively applied to these three sections allowed obtaining laser wavelength tuning without changes of the optical power or power modulation without emission wavelength shifts. Pure FM was achieved by simultaneously modulating the currents of the master oscillator and phase sections, whereas pure AM was obtained by modulating only the phase section.

In this article, we present a different approach to generate electrically either pure FM or pure AM in a QCL. It makes use of a new feature that has been recently introduced in QCLs in the form of an integrated heater (IH) located in the vicinity of the active region (AR) in a distributed feedback (DFB) QCL [27]. This resistive heater enables controlling the internal temperature of the AR by Joule's dissipation via an electrical current, which is much faster than standard temperature control with a thermo-electrical cooler [28]. Changing the temperature of a QCL modifies both its frequency and its output power. Therefore, the IH simultaneously acts on these two quantities. The IH current affects the QCL optical frequency in the same way as the AR current (i.e., the optical frequency decreases with increasing current), as both current tunings result from a thermal effect. However, the optical power of the QCL decreases with increasing IH current (as the laser threshold current increases with temperature), whereas it increases with the AR current. Therefore, a modulation applied to the AR and IH currents has a different effect on the laser AM and FM. Combining a simultaneous modulation of the two currents with an appropriate relative amplitude and phase can enable suppressing either the AM (thus producing pure FM) or the FM (thus generating pure AM). We demonstrate these two situations in a QCL emitting at 7.8 µm, and show a reduction of the parasitic modulation by almost two orders of magnitude compared to the usual case where only the AR current is modulated. This high reduction of the parasitic modulation is presented at two characteristic frequencies of 1 and 10 kHz for proof-of-principle demonstration. Our results incorporate a study of the dynamic response of the output power and emission frequency of the QCL for the two applied modulation signals and show how their relative amplitude and phase must be adjusted as a function of the considered modulation frequency.

2. Experimental setup and methods

The laser used in this work is a DFB-QCL emitting at 7.8 µm and equipped with an IH with an internal resistance of ~5.6 Ω located a few micrometers from the AR. It is of the same type as initially reported by Bismuto *et al*. [27] and later on extensively characterized by Gürel *et al*. in terms of tuning speed and modulation transfer functions [28]. The QCL soldered on a copper sub-mount was placed in a standard laser laboratory housing (LLH) from Alpes Lasers and temperature-stabilized near 25°C by a thermo-electrical cooler. The static tuning curves and output power of the QCL measured at this temperature as a function of the AR and IH currents are shown in Fig. 1. The static tuning coefficients are typically −0.55 GHz/mA as a function of the AR current (similar to values previously reported for standard DFB-QCLs at this wavelength [29]) and −23.95 GHz/W as a function of the electrical power dissipated in the IH. The tuning curves were determined from the position of several N_2O absorption lines measured in a low-pressure (2 mbar) gas cell in correspondence to their reference values from the HITRAN spectroscopic database [30]. The output power was measured using a thermal powermeter placed in front of the laser housing after an external collimating lens. As a result of the high divergence of the light beam at the output of the QCL and the limited numerical aperture of the lens, only part of the total emitted power was detected in this case. This had no impact on the measurement reported here as the purpose was only to observe the relative variation of the optical power as a function of the current in the AR or IH, respectively. The

Optics EXPRESS

result shows that the optical power increases with the current in the AR (up to the roll-over current). On the contrary, it decreases with the IH current, which induces a heating of the laser AR that leads to an increase of the threshold current and an associated power reduction at constant AR current. At the same time, the frequency of the emitted light decreases with both currents due to their predominant thermal effect. This dependence is fairly linear with respect to the AR current, but has a higher quadratic component for the IH current as the electrical power dissipated in the IH scales with the squared current.

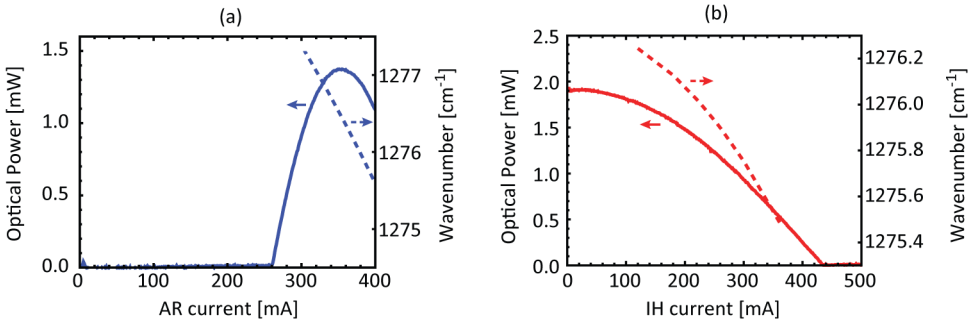

Fig. 1. Output power (solid lines, left axis) and emission wavenumber (dashed lines, right axis) of the QCL measured as a function of the AR current I_{AR} (a) and of the IH current I_{IH} (b). The QCL heat-sink temperature was 25 °C in all cases. In (a), I_{IH} = 250 mA; in (b), I_{AR} = 320 mA.

The QCL AR and IH were driven by two distinct home-made low-noise current sources. The output beam of the laser was split into two paths by a beamsplitter plate with a nominal splitting ratio of 50/50 (however, it was closer to 60% reflection and 40% transmission at our wavelength and for the considered laser polarization). A photodiode (PD-1 in Fig. 2) measured the AM in the first path. A low-pressure (2 mbar) 10-cm long N_2O gas cell was used in the second path to measure the FM of the laser. The QCL frequency was tuned to the flank of a strong N_2O absorption line at 1277 cm^{-1} used as frequency discriminator to convert FM into intensity modulation, which was detected by a second photodiode (PD-2 in Fig. 2). A typical discriminator slope $D \approx$ -7.9 V/GHz was measured for a total contrast of the N_2O absorption line of ~1.2 V as shown in Fig. 2. Owing to the steep slope of the absorption line, the measured signal of PD-2 was dominated by the laser FM and the direct contribution of the laser AM was negligible. The AM and FM transfer functions were measured by applying a sine modulation to the current driver of the IH or AR and by demodulating the signal of both detectors (PD-1 for AM, PD-2 for FM) in amplitude and phase using a lock-in amplifier (Zurich Instruments HF2LI) referenced to the applied modulation signal. The modulation frequency f was changed between 1 Hz and 1 MHz (10 points per decade, equally-spaced in a logarithmic scale) and the corresponding amplitudes and phases were recorded. The drivers have a typical modulation bandwidth in the range of 1 MHz and a modulation coefficient of 2 mA/V. The transfer functions were obtained by normalizing the measured lock-in signals by the applied current modulation amplitude. For FM, the discriminator slope was taken into account to convert the detector signal into a change of the optical frequency to get the FM response in GHz/mA. For AM, the relative power modulation was calculated by normalizing the lock-in signal by the average detector output voltage in order to retrieve the relative AM response in %/mA.

Optics EXPRESS

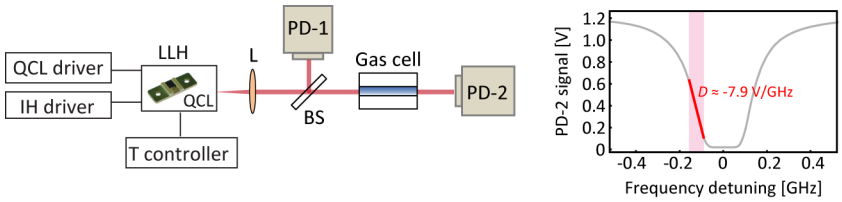

Fig. 2. Schematic of the experimental setup used to characterize the AM and FM properties of the IH-QCL. Photodiode PD-1 directly measures the AM of the laser, while photodiode PD-2 measures the FM by means of an optical frequency discriminator made of a molecular absorption line in a spectroscopic setup. LLH: laser laboratory housing; L: collimating lens; BS: beamsplitter plate. Right: transmission profile of the P9 absorption line in the ν_3 vibrational band of N_2O at 1277.2 cm^{-1} used as frequency discriminator with a measured slope $D \approx -7.9$ V/GHz (red line). The linear range on the side of the absorption line in which the laser FM can be measured without distortion is indicated by the colored area.

3. Experimental results

3.1 Modulation transfer functions

The transfer functions measured for a modulation of the current applied to the AR or IH around their average values of I_{AR} = 320 mA and I_{IH} = 250 mA, respectively, are displayed in Fig. 3. The FM transfer functions (dashed lines) are very comparable to those previously reported for a similar IH-QCL [28]. They are characterized by different time constants that result from the heat extraction in different areas of the laser. The FM bandwidth is larger for a modulation of the current in the AR, as the heat is directly produced in the gain medium. The AM transfer function is also significantly different for a modulation of the IH or AR current. The AM response is almost constant up to a modulation frequency close to 1 MHz for the AR current, which seems to be limited by the bandwidth of the driver. For a modulation of the IH current, the response drops much faster, resulting from the fact that the power variations induced by the IH current arise from a thermal effect that is limited in bandwidth.

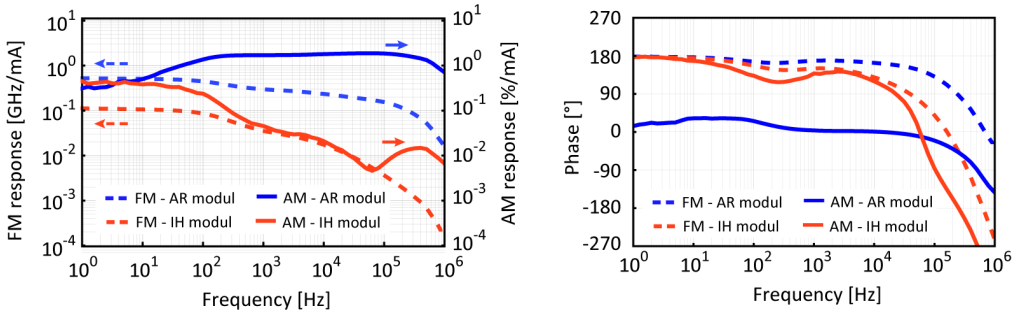

Fig. 3. Amplitude (left) and phase (right) of the AM (solid lines) and FM (dashed lines) transfer functions measured for a modulation of the current of the AR (blue) and IH (red) around their average values of I_{AR} = 320 mA and I_{IH} = 250 mA.

Hence, the ratio H_{IH} /H_{AR} of the amplitude of the transfer functions obtained for a modulation of the IH and AR currents (either for FM or AM) has a strong frequency dependence as displayed in Fig. 4. The relative phase shift $\varphi_{IH\text{-}AR} = \varphi_{IH} - \varphi_{AR}$ is also frequency dependent, where φ_{IH} and φ_{AR} are the phase of the individual transfer functions displayed in Fig. 3. The modulation of the two currents leads to a similar phase (at low modulation frequencies) of the FM transfer functions, but to an opposite phase for AM. Therefore, applying a simultaneous modulation to the AR and IH currents with a suitable relative amplitude and phase shift can result in a compensation of the two AM (resp. FM) contributions, leading to the possibility to produce pure FM (resp. AM).

Optics EXPRESS

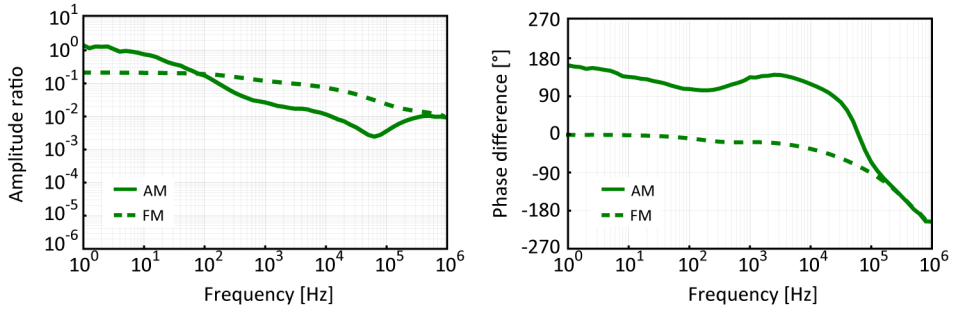

Fig. 4. Amplitude ratio H_{IH} /H_{AR} (left) and phase shift $\varphi_{IH\text{-}AR}$ (right) between the transfer functions obtained for a modulation of the IH and AR currents in the case of AM (solid line) and FM (dashed line) at an operation point of the laser characterized by I_{AR} = 320 mA and I_{IH} = 250 mA.

3.2 Pure AM

The generation of a pure AM signal is illustrated in Fig. 5 in the particular case of modulation frequencies of 1 kHz and 10 kHz chosen for the proof-of-concept demonstration of the dual modulation method. However, similar results can be achieved at other modulation frequencies following the same principle. The temporal traces of the individual AM and FM signals produced when modulating either the AR current (blue lines) or the IH current (red lines) alone are displayed together with their combination (green lines) resulting into pure AM. The applied AM is relatively small here (<1%). It was limited in this example by the measurement of the FM signal produced by the AR or IH current modulation using the N_2O frequency discriminator. The linear range of the N_2O absorption line in which the FM can be measured without distortion is restricted to less than ~60 MHz (see colored area in Fig. 2), corresponding to a change of the AR current smaller than 0.1 mA at low modulation frequency (< 100 Hz) and ~0.5 mA at f = 200 kHz. The modulation signals applied to the AR and IH induce an FM depth in this range as shown in Fig. 5.

The value of the amplitude ratio ΔI_{AR} / ΔI_{IH} and phase shift $\phi_{IH\text{-}AR}$ between the two modulation signals to be applied for efficient FM reduction depends on the operating points (average current) of the AR and IH sections. Both parameters furthermore depend on frequency as previously shown by the frequency dependence of the relative phase shift $\varphi_{IH\text{-}AR}$ observed in Fig. 4. Therefore, these parameters must be precisely determined at the considered operation point of the laser and for the modulation frequency of interest. The phase difference $\phi_{IH\text{-}AR} = \phi_{IH} - \phi_{AR}$ between the two control signals $I_{IH}(t) = \Delta I_{IH} \sin(2\pi ft + \phi_{IH})$ and $I_{AR}(t) = \Delta I_{AR} \sin(2\pi ft + \phi_{AR})$ at frequency f applied to the current drivers must be adjusted such that the total phase between the two induced modulation signals is equal to 180° for the modulation to be suppressed, in this case FM: $\phi_{IH\text{-}AR}^{FM} + \varphi_{IH\text{-}AR}^{FM} = 180°$. This total phase is the combination of the phase shift $\phi_{IH\text{-}AR}$ between the two applied current modulation signals and the phase difference $\varphi_{IH\text{-}AR}$ resulting from the laser response. Then, the relative amplitude ΔI_{AR} / ΔI_{IH} of the two modulation signals must be adjusted to compensate for the different response of the laser to these modulations, which is characterized by the amplitude ratio H_{IH}/H_{AR} of the transfer functions displayed in Fig. 4, i.e., one must have ΔI_{AR} / ΔI_{IH} = H_{IH} / H_{AR}.

Optics EXPRESS

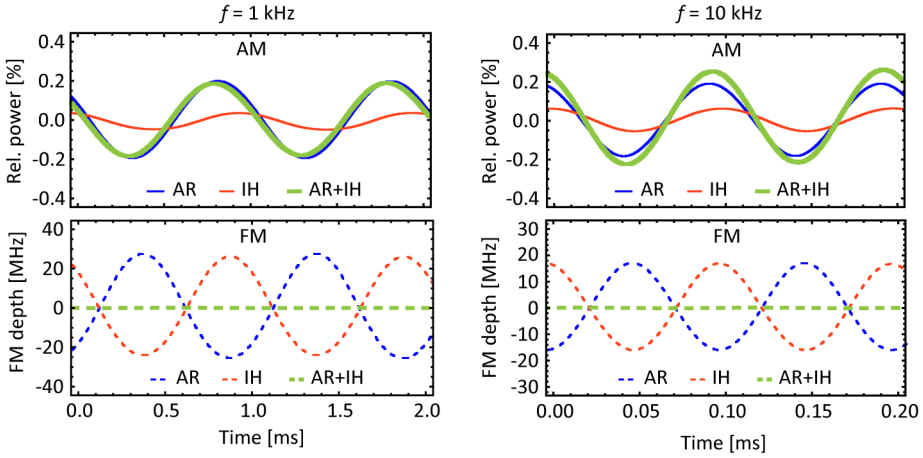

Fig. 5. Examples of single-channel AM (top) and FM (bottom) signals resulting from a modulation of the AR current (blue curves) or of the IH current (red curves); combined AM (solid green curves) and FM (dashed green curves) modulation signals obtained for maximum FM suppression (pure AM). The left and right graphs correspond to a modulation frequency f of 1 kHz and 10 kHz, respectively. The amplitude of the applied modulation signals is 50 mV to the AR driver in all cases (resulting in ΔI_{AR} = 0.1 mA), 415 mV at 1 kHz and 680 mV at 10 kHz to the IH driver (corresponding to 0.83 mA and 1.36 mA, respectively).

At a modulation frequency of 1 kHz, the relative FM induced by the IH and AR currents is characterized by $H_{IH}^{FM}/H_{AR}^{FM} = 0.118$ and $\varphi_{IH\text{-}AR}^{FM} = -18.3°$. Pure AM is therefore expected to be achieved by applying two modulation signals such that $\Delta I_{AR}/\Delta I_{IH}$ = 0.118 and $\phi_{IH\text{-}AR} = 198.3°$. These parameters become $\Delta I_{AR}/\Delta I_{IH} = 0.074$ and $\phi_{IH\text{-}AR} = 215°$ at 10 kHz. The resulting FM signal has been recorded as a function of the relative ratio and phase shift between the two modulations to assess the sensitivity of their adjustment for a proper FM suppression. A fixed modulation signal of 200 mV at 1 kHz or 145 mV at 10 kHz was applied to the current driver controlling the laser AR, corresponding to a current modulation amplitude of 0.4 mA (at 1 kHz) or 0.29 mA (at 10 kHz) in the AR. These values are higher than the upper limit mentioned in the beginning of Section 3.2 for a correct measurement of the FM signal. However, it does not affect the results reported here as we are interested in the small total FM signal resulting from the combined modulation of the AR and IH currents and not in the stronger individual FM signals that may be distorted at this modulation amplitude.

A signal generator (HP 3314A) was used to modulate the IH driver. The generator was phase-locked to the modulation signal applied to the AR and delivered an output signal with a varying phase and amplitude to modulate the IH driver. The phase of the applied signal was scanned over a range of more than 60° with a step of 1° for a series of different amplitudes and the resulting FM signal (from photodiode PD-2) was measured by the lock-in amplifier with a time constant of 0.7 s for 1-kHz modulation and 0.3 s for 10-kHz modulation. The second channel of the lock-in amplifier was used to precisely measure the phase of the applied modulation signal in comparison to the AR modulation, i.e., the phase difference $\phi_{IH\text{-}AR}$. The different sets of experimental data were processed together to calculate the density plots displayed in Fig. 6, which show the reduction of the FM signal from the case where a modulation is applied to the AR only. The highest FM suppression is achieved for $\Delta I_{IH} = 3.4$ mA (i.e., $\Delta I_{AR}/\Delta I_{IH} \approx 0.117$) and $\phi_{IH\text{-}AR} \approx 199°$ at f = 1 kHz, and ΔI_{IH} = 4 mA ($\Delta I_{AR}/\Delta I_{IH} \approx 0.072$) and $\phi_{IH\text{-}AR} \approx 214°$ at f = 10 kHz, in good agreement with the values extracted from the amplitude ratio and phase difference of the transfer functions displayed in Fig. 4 ($H_{IH}^{AM}/H_{AR}^{AM} = 0.118$ and $\varphi_{IH\text{-}AR}^{AM} = -18.3°$ at f = 1 kHz, $H_{IH}^{AM}/H_{AR}^{AM} = 0.074$ and $\varphi_{IH\text{-}AR}^{AM} = -34.2°$ at f = 10 kHz). A reduction of the FM by more than two orders of magnitude

Optics EXPRESS

is demonstrated at both modulation frequencies of 1 kHz (>24 dB) and 10 kHz (>22 dB) when using the combined modulation with optimized parameters in comparison to the traditional modulation applied to the QCL current only. These values may be slightly underestimated as the maximum FM depth obtained for a modulation of the AR current only and used in the normalization of the recorded data to determine the FM attenuation is larger than the linear range of the N_2O frequency discriminator. Therefore, the determined normalization FM signal is slightly lower than in reality (we estimated the resulting signal reduction to be around 40%), which should lead to an effective FM attenuation that is still enhanced by around 2 dB from the aforementioned values.

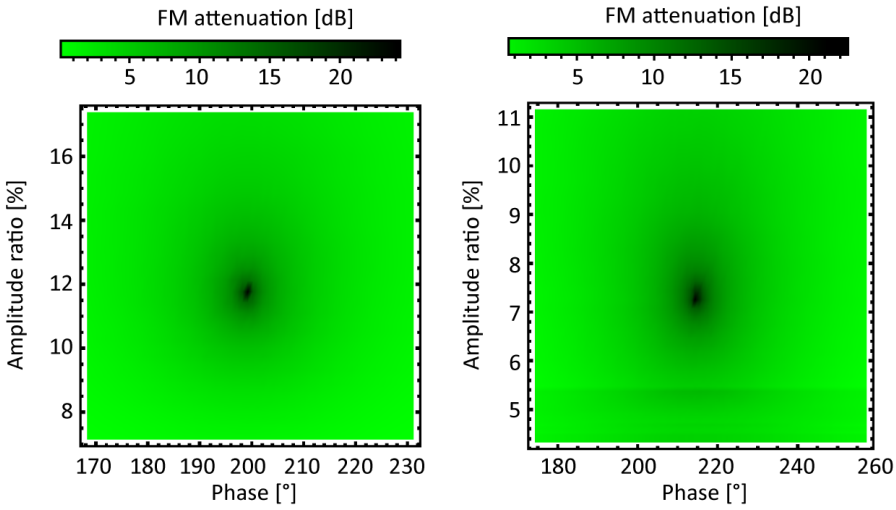

Fig. 6. Density plot showing the reduction of the residual FM signal as a function of the amplitude ratio and phase shift between the modulation signals applied to the IH and AR currents, in comparison to the FM signal arising when only the AR current is modulated. The left and right graphs correspond to a modulation frequency of 1 kHz and 10 kHz, respectively. A modulation signal with an amplitude of 200 mV was applied to the AR driver at f = 1 kHz, and 145 mV at f = 10 kHz (resulting in ΔI_{AR} = 0.4 mA and ΔI_{AR} = 0.29 mA, respectively).

3.3 Pure FM

For pure FM, the same setup and procedure were used. The amplitude ratio and phase shift between the two modulations were adjusted in order to minimize the residual AM signal. Figure 7 displays the corresponding temporal traces of the individual AM and FM signals obtained when modulating either the AR current (blue lines) or the IH current (red lines) alone at 1 kHz or 10 kHz, together with their combination (green lines) resulting into a pure FM. The modulation signals applied to the AR and IH were kept small enough to ensure that the total induced FM could be correctly measured using the N_2O frequency discriminator. Therefore, the FM depth produced in these examples is smaller than 100 MHz. However, larger amplitudes can be obtained in principle while keeping an efficient suppression of the parasitic AM by increasing the amplitude of the two modulation signals by the same factor to keep their ratio constant. Due to the small modulation signal used here, the corresponding residual AM time traces were fairly small and could not be directly observed on an oscilloscope. Therefore, 128 traces were averaged on the scope to improve the signal-to-noise ratio and the resulting averaged curves are displayed in Fig. 7. We also noticed that these time traces could vary from measurement to measurement due to some possible optical feedback to the QCL (there is no optical isolator in the experimental setup). Therefore the small residual modulation observed in the AM time traces may partially result from optical feedback and is not necessary the residual AM signal arising from the applied modulation signals.

Optics EXPRESS

The residual AM signal was measured as a function of the amplitude ratio and phase shift between the two applied modulations at the two characteristic frequencies of 1 and 10 kHz by lock-in detection with a time constant of 0.7 s for 1-kHz modulation and 0.3 s for 10-kHz modulation. A fixed modulation signal of 160 mV (at f = 1 kHz) or 80 mV (at f = 10 kHz) was applied to the current driver controlling the laser AR, corresponding to a current modulation amplitude of 0.32 mA (1 kHz) or 0.16 mA (10 kHz) in the AR. The signal applied to the IH was scanned in amplitude and phase as previously described for the pure AM case. The individual FM signals induced by the modulation of the AR and IH currents are slightly larger than previously stated to stay in the linear range of the N_2O frequency discriminator, but it does not impact the measurement as the purpose here was to measure the residual AM signal that is not affected by this limitation.

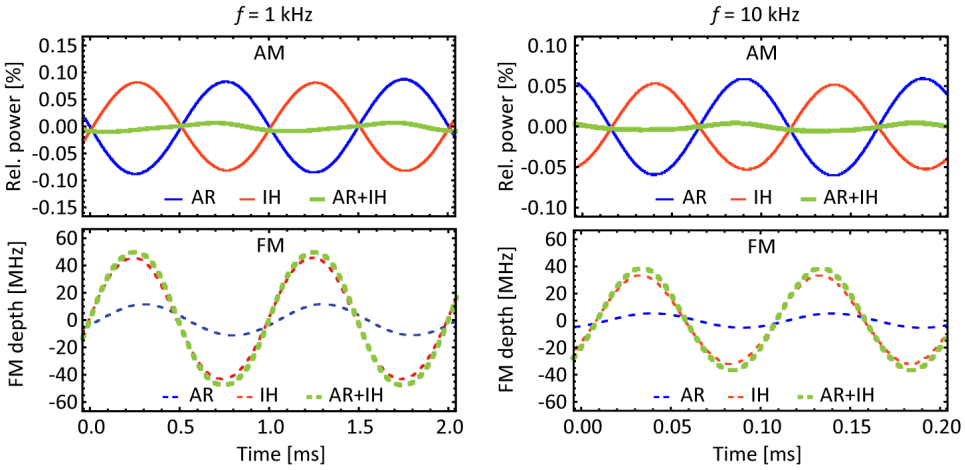

Fig. 7. Examples of single-channel AM (top) and FM (bottom) signals resulting from a modulation of the AR current (blue curves) or of the IH current (red curves); combined AM (solid green curves) and FM (dashed green curves) modulation signals obtained for maximum AM suppression (pure FM). Due to the small amplitude of the AM time traces, these curves were recorded with 128 averages on the scope. The left and right graphs correspond to a modulation frequency f of 1 kHz and 10 kHz, respectively. The amplitude of the applied modulation signals is 22 mV (at 1 kHz) or 15 mV (10 kHz) to the AR driver (resulting in ΔI_{AR} = 0.044 mA or 0.03 mA, respectively) and 810 mV at 1 kHz and 1.2 V at 10 kHz to the IH driver (corresponding to 1.62 mA and 2.4 mA, respectively).

The optimal AM suppression is achieved for $\Delta I_{AR}/\Delta I_{IH} \approx 0.027$ and $\phi_{IH\text{-}AR} \approx 48°$ at a modulation frequency of 1 kHz and $\Delta I_{AR}/\Delta I_{IH} \approx 0.012$ and $\phi_{IH\text{-}AR} \approx 60°$ at 10 kHz. These values are in excellent agreement with the parameters assessed from the relative AM transfer function displayed in Fig. 4 ($H_{IH}^{AM}/H_{AR}^{AM} = 0.027$ and $\varphi_{IH\text{-}AR}^{AM} = 134.7°$ at f = 1 kHz; $H_{IH}^{AM}/H_{AR}^{AM} = 0.012$ and $\varphi_{IH\text{-}AR}^{AM} = 118.9°$ at f = 10 kHz). Here also, a reduction of the AM by almost two orders of magnitude is demonstrated at both modulation frequencies of 1 kHz (>21 dB) and 10 kHz (>18 dB) with the combined modulation in comparison to the traditional modulation applied to the QCL current only. The lock-in detection scheme applied here really measures the residual AM signal occurring at the applied modulation frequency f and is not sensitive to other spurious AM that may be present as observed in the time traces of Fig. 8, which may partially result from optical feedback.

Optics EXPRESS

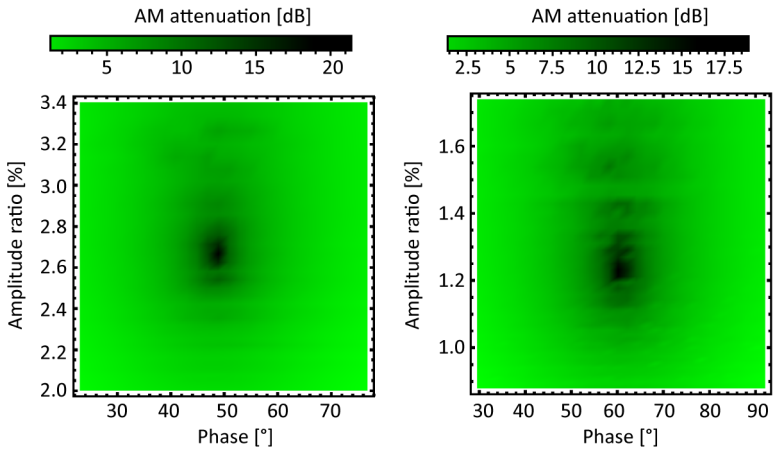

Fig. 8. Density plot showing the reduction of the residual AM signal as a function of the amplitude ratio and phase shift between the modulation signals applied to the IH and AR currents, in comparison to the AM signal arising when only the AR current is modulated. The left and right graphs correspond to a modulation frequency of 1 kHz and 10 kHz, respectively. A modulation signal with an amplitude of 160 mV was applied to the AR driver at f = 1 kHz and 80 mV at f = 10 kHz (resulting in ΔI_{AR} = 0.32 mA and ΔI_{AR} = 0.16 mA, respectively).

3.4 Discussion

The results reported in Sections 3.2 and 3.3 were obtained at a given operation point of the QCL (average AR and IH currents, and heat-sink temperature). The parameters of the applied modulation signals to achieve either pure AM or pure FM depend on the operation point of the QCL, i.e., mainly on the value of the AR and IH currents. For instance, the modulation properties of the laser for a modulation of the IH current strongly depend on the average IH current I_{IH} due to the nonlinear response of the QCL power and wavelength as a function of this parameter [28]. The influence of the QCL temperature is much smaller. However, a slight adjustment of the modulation parameters might be needed to maintain an efficient suppression of the AM or FM when changing the QCL temperature via its thermo-electrical cooler. This is also the case when changing the QCL AR current. More important variations of the optimized modulation parameters occur when operating the QCL at a different IH current. However, the same suppression efficiency of the spurious modulation is expected regardless of the QCL operating point, provided that the modulation parameters are properly determined from the ratio and phase shift of the transfer functions, as exemplified in this work at two particular modulation frequencies.

It is also frequent in spectroscopic sensing applications, notably with QCLs, that the AR current is not only modulated at a frequency f (sine modulation), but is additionally slowly ramped (triangular modulation at a much lower frequency f_{scan}) in order to scan the modulated laser radiation through an absorption line of the analyzed gas species (e.g., in WMS). For the aforementioned reason, the AM and FM responses of the laser to the fast AR current modulation at frequency f may slightly change during the scan, which may affect the AM or FM suppression. However, the used scan amplitude is usually limited. With a typically tuning coefficient of ~0.5 GHz/mA for QCLs in the 8-µm range, a current ramp of ± 10 mA enables scanning the laser over 10 GHz, which is generally sufficient in most sensing applications of small molecules. In a QCL, the FM coefficient changes with the AR current; we previously measured a variation of around 50% in a current range of 300 mA in DFB-QCLs at 7.8 µm [29], corresponding to a relative change of less than 0.15%/mA. Over a current range of ± 10 mA, the corresponding overall change of the FM signal would be only ~3%. Therefore, a high suppression of the FM signal would still be obtained during the AR current scan when applying a constant modulation signal to the IH. The FM suppression would likely not reach

Optics EXPRESS

~20 dB as demonstrated in this work at a constant AR current, but values in the range of 15 dB appear still feasible, which is already a high suppression. Furthermore, a small AM (at the slow ramp frequency) could be added to the carrier signal applied to the IH to mitigate this effect by slightly changing the amplitude of the IH modulation signal during the slow scan. This can easily be done when generating the modulation signals with a digital system.

Similarly, the AM signal produced by AR current modulation may depend on the mean AR current and can thus vary during a current scan. For the same reason as explained before, the amplitude of this scan is usually limited to typically ± 10 mA. If the laser is operated in the perfectly linear range of its light-vs-current (LI) curve, the amplitude of the AM signal would be independent of the average AR current (the relative AM varies but the absolute AM signal remains constant). In that case, scanning the AR current is not expected to affect the AM suppression in pure FM applications. In reality, the LI curve of a QCL presents some nonlinearity and even a reversal point at the roll-over current as visible in Fig. 1(a). If the laser is operated in the nonlinear range, the small nonlinearity induces a change of the AM signal when scanning the AR current. However, this change remains moderate if the laser is operated far enough from the roll-over current and the current scan amplitude is kept small. As for the case of pure AM discussed before, the AM suppression would likely not reach the ~20 dB demonstrated here at a constant AR current, but 15 dB appear still feasible, which is already a high suppression.,

4. Conclusion

We have demonstrated an all-electrical method to produce either pure FM or AM in a QCL by applying modulation signals of proper amplitude and phase to two different actuators. The QCL injection current and the current in an IH enable the temperature of the laser active region to be controlled with a relatively high speed. A detailed analysis of the residual modulation has been performed at two characteristic frequencies of 1 and 10 kHz, showing a reduction of the AM by almost two orders of magnitude and of the FM by more than 20 dB in comparison to the traditional modulation applied to the QCL current only. Similar results can be obtained at other modulation frequencies by a proper adjustment of the relative amplitude and phase of the two applied modulation signals. We have shown how these parameters can be obtained with a good accuracy from the measured transfer functions.

The proposed approach is attractive for enhanced performance in sensing methods in which the spurious residual modulation constitutes a parasitic effect that impacts the performance. This is for instance the case for spectroscopic trace gas sensing in which either pure FM or pure AM is generally desired. It is difficult to quantify here the effective benefit that the proposed approach can bring in terms of detection sensitivity as it strongly depends on the considered situation. For instance, the impact of RAM is much detrimental if the laser is operated close to the threshold current than far above. However, the benefit of reducing the RAM in WMS was clearly shown for instance with the use of near-infrared laser diodes [31].

Funding

Swiss National Science Foundation (SNSF) (200020_166104, 200020_178864); Swiss Confederation Program Nano-Tera.ch, scientifically evaluated by the SNSF (IRsens-2); European Space Agency (ESA) (4000117741/16/NL).